

The Influence of Mutation at Glu44 and Glu56 of Cytochrome *b*₅ on the Protein's Stabilization and Interaction between Cytochrome *c* and Cytochrome *b*₅[†]

Wen Qian, Yu-Long Sun, Yun-Hua Wang, Ji-Hua Zhuang, Yi Xie, and Zhong-Xian Huang*

Department of Chemistry, Fudan University, Shanghai 200433, China

Received March 3, 1998; Revised Manuscript Received July 27, 1998

ABSTRACT: To characterize the roles played by Glu44 and Glu56 of cytochrome *b*₅ in the formation of the electrostatic complex between cytochrome *c* and cytochrome *b*₅, the Glu44, Glu56, or both sites were changed to alanine by site-directed mutagenesis. The influence of these two residues on the protein stability was probed by investigating the kinetic behaviors of protein denaturation in urea or upon heating and the heme-transfer reactions between apo-myoglobin and the variants of cytochrome *b*₅. It has been found that when the Glu44 and/or Glu56 are mutated to alanine, the protein stability increases slightly due to the fact that the hydrophilic residue is changed to a hydrophobic one, resulting in the two pairs of helices surrounding the heme taking a more compact conformation. The difference in voltammetric behavior of cytochrome *c*, cytochrome *b*₅, and its three mutants, Cyt *b*₅ E44A, E56A, and E44/56A, alone and in 1:1 protein complexes demonstrates that both Glu44 and Glu56 of cytochrome *b*₅ take part in the electrostatic interaction with cytochrome *c*. The entropy changes, $\Delta S^\circ_{\text{rc}}$ and enthalpy changes, ΔH° , derived from the temperature dependence of the formal reduction potentials of each protein in different protein systems suggest that, because of the mutual interaction with cytochrome *c*, cytochrome *b*₅ mutants, especially the E44A-containing mutants, in the protein complexes suffer greater conformational changes upon reduction than that of the wild type. The variation of these thermodynamic parameters indicates that the strength of mutual interactions between cytochrome *c* and cytochrome *b*₅ or its mutants has the following order: Cyt *c*/Cyt *b*₅ > Cyt *c*/Cyt *b*₅ E56A > Cyt *c*/Cyt *b*₅ E44A > Cyt *c*/Cyt *b*₅ E44/56A.

Cytochrome *b*₅ (Cyt *b*₅) is found both as a component of the microsomal membranes and as a soluble form in erythrocytes. The microsomal protein plays an important role in fatty acid desaturation (1) and in the cytochrome P-450 reductase system (2), while the soluble form acts as an electron mediator in the erythrocyte methemoglobin reduction system (3). Microsomal cytochrome *b*₅ consists of a water-soluble, heme-binding domain and a short hydrophobic domain of approximately 40 amino acid residues that serves to anchor the protein to the microsomal membrane (4). The water-soluble domain is readily released from the microsomal membranes by mild proteolysis (5) and retains full activity of the cytochrome *b*₅ (6–7). The heme-containing fragment has been the subject of intensive investigation. X-ray crystallographic studies of the water-soluble lipase-cleaved fragment of bovine liver microsomal cytochrome *b*₅ have revealed a compact, cylindrical molecule containing six α -helices and five β -strands (8–9) which constitute a hydrophobic heme-binding pocket. The heme itself has two anionic propionates; one projects out into the solvent, and the other folds back into the protein interior. There are 11 conserved glutamate and aspartate residues surrounding the heme-exposed edge on the surface of cytochrome *b*₅, which was suggested as the binding domain

for the positively charged reactive partners. The static juxtaposition of oppositely charged surfaces stabilizes the binary complexes, which was supported by the computer simulation of the interaction of cytochrome *b*₅ with cytochrome *c* (10), cytochrome P-450 (11), methemoglobin α domain (12), methemoglobin β -chain (13), methemerythrin chain (13), and metmyoglobin (14).

The surface negatively charged residues, Glu44 and/or Glu56 of cytochrome *b*₅, were suggested to participate in the formation of a salt bridge with cytochrome *c* (10, 15–18). To examine the structural and functional importance of Glu44 and Glu56, in the present study, a site-directed mutagenesis system was employed to generate cytochrome *b*₅ mutants in which the Glu44 and Glu56 were mutated to alanine. The relative stability of these proteins to denaturant and heat was determined. At the same time, the heme-transfer reactions between cytochrome *b*₅ or its mutants and apo-myoglobin were also studied. The results show that when the Glu44 and Glu56 are mutated to alanine, the stability of cytochrome *b*₅ increases. Whether the changes in protein stability affect the mutual interaction between cytochrome *c* and cytochrome *b*₅ requires further investigation.

For redox metalloproteins, electrochemistry is one of the most powerful tools in probing and evaluating the structure, function, and mechanism of the protein. The direct electrochemical measurements of reduction potentials have been achieved for redox active sites in low molecular weight electron-transfer proteins (19–21). In a series of electro-

[†] This project is supported by the National Natural Science Foundation of China, the State Key Laboratory of Genetics of Fudan University, and the State Key Laboratory of Bio-organic Chemistry of the Shanghai Institute Of Organic Chemistry, the Chinese Academy of Science.

* To whom all correspondence should be addressed.

chemical studies on cytochromes we have reported that (1) the electrochemistry of horse heart cytochrome *c* has been effectively promoted by some amino acids at a gold electrode, and a good, quasi-reversible redox reaction has been achieved (22). (2) On the amino acid-modified electrode there is no electrochemical response to the negatively charged protein, cytochrome *b*₅; however, a near-reversible cyclic voltammetric response of cytochrome *b*₅ or its mutants, E44A, E56A, and E44/56A, has been observed at a gold electrode modified with thioglycolic acid through the promotion of the multivalent cations such as Mg²⁺ or Cr(NH₃)₆³⁺ ions (23). (3) The direct electrochemistry of the cytochrome *c*, cytochrome *b*₅, and Cyt *c*/Cyt *b*₅ complex system has been investigated by cyclic voltammetry at a cysteine-modified gold electrode. This functional electrode can selectively permit a quasi-reversible electrochemical response of cytochrome *c* only, whereas a near-reversible electrochemical response of cytochrome *b*₅ stimulated by Mg²⁺ ion can be simultaneously observed. From titration experiments, formation of a 1:1 Cyt *c*/Cyt *b*₅ protein complex has been observed in the presence of Mg²⁺ ion, and the Mg²⁺ ion exerts a stronger effect on the electrochemical behavior of cytochrome *c* than that of cytochrome *b*₅. We hypothesized that there were different interaction models between cytochrome *c*, cytochrome *b*₅ or the 1:1 protein complex, and the electrode (24–25). As we know, the wide range of entropy variations of the low molecular weight complexes in aqueous solution undoubtedly relies on the nature of the oxidized and reduced metal centers and the structure of the ligands, as well as the specific solvent structure and charges surrounding the complex (26–27). For the redox systems consisting of a metal center and macromolecule ligands such as metalloproteins, it is anticipated that the entropy values predominantly reflect the ligand rather than metal characteristics. The enthalpies and entropies of metalloprotein electron-transfer reaction are dominated by changes in protein's conformation and solvation as indicated by Anson and Gray (28–29). Most importantly, the entropy changes tightly relate to the ligand's (protein's) structure, conformation, and the reorganization (including both the protein and the surrounding water molecules) on change in redox state. Therefore, it will be most valuable to estimate the entropic driving forces for the redox protein reactions besides the knowledge obtained from the free energies alone.

In this paper, we also described our further study on the cyclic voltammetric behaviors of cytochrome *c*, cytochrome *b*₅, and its three mutants alone, as well as the different Cyt *c*/Cyt *b*₅ complex systems at varied temperature. The formal reduction potentials were determined by cyclic voltammetry at a cysteine-modified gold electrode, which provides accurate estimates of the formal reduction potentials for the metalloproteins (30). On the basis of the above considerations, we focused our study on the thermodynamic parameters, especially on their entropy changes of each protein alone and in the 1:1 protein complexes formed by cytochrome *c* and cytochrome *b*₅ or its mutants. The entropy changes should mainly reflect the changes in structure and conformation of each macromolecular ligand in the formation of 1:1 protein complexes.

It is a moot point whether Glu44 and/or Glu56 are involved in the formation of the cytochrome *c*/cytochrome *b*₅ complex. One aim of this study is to provide convincing evidence to

elucidate the role of the acidic side chains surrounding the heme-exposed edge of cytochrome *b*₅ and their influence on the interaction with cytochrome *c*. The detailed information obtained from electrochemical measurements allows us to gain a deeper understanding of the structural factors and the mutual interaction between two proteins that influence the thermodynamics of redox processes. The striking results obtained support the conclusion that both Glu44 and Glu56 of cytochrome *b*₅ participate in the formation of 1:1 cytochrome *c*/cytochrome *b*₅ complex.

EXPERIMENTAL SECTION

Materials. Horse heart cytochrome *c*, type VI, was purchased from Sigma and purified by ion-exchange chromatography using carboxymethyl-cellulose resin (CM-52, Whatman Biochemicals Ltd) (31–32). Hepes (4-(2-hydroxyethyl)-1-piperazineethane-sulfonic acid) was purchased from Farco Chemical Supplies. The surface modifier, L-cysteine, was obtained from BDH as the hydrochloride salt. All other reagents were of analytical quality. Protein solutions of known concentrations were prepared in Hepes buffer (1 mM, pH 7.0) containing 20 mM KCl to keep the ionic strength and 4 mM Mg²⁺ ion to stimulate the quasi-reversible voltammetric responses of the proteins studied.

Protein Preparations. The generation and purification of variant forms of cytochrome *b*₅ have also been described previously (33). Mutagenesis was performed using a M13mp18 phagemid carrying a gene copy of the trypsin-solubilized bovine liver microsomal cytochrome *b*₅. Mutated plasmids were identified by sequencing the single-stranded DNA and double-stranded DNA using the Sanger dideoxy procedure (34). The accuracy of all mutant constructs was also verified by analysis of amino acid compositions and electrospray mass spectrometry.

Thermostability of Cytochrome *b*₅ and Its Mutants. Cytochrome *b*₅ or its E44A, E56A, and E44/56A mutants were dissolved in the phosphate buffer (100 mM, pH 7.0), respectively. The protein concentration was about 6 μM. The protein sample was placed in a water-jacketed quartz cell (10 mm path length). At each given temperature the protein solution was allowed to equilibrate for at least 15 min until the absorbance reading at 412 nm was stable before the spectrum was recorded. The temperature was increased stepwise in the region of 25–90 °C. The temperature accuracy was within ± 0.2 °C.

pH Effect on the Structural Stability of Cytochrome *b*₅ and Its Mutants. After equal volumes of protein solution were mixed with different pH phosphate buffer solutions (1 M, pH 2–5), the mixture was left at room temperature for 5 h. The pH of the protein solution was measured by a pHs-3 meter. The spectra of the protein solutions at different pH were recorded on a HP8452A UV–vis spectrophotometer using a phosphate buffer as a reference.

Heme-Transfer Reaction between Cytochrome *b*₅ and Apo-myoglobin. Apo-myoglobin was prepared as previously described (35) and solved in 1 mM sodium phosphate, pH 6.8, and 1.5 mL of apo-myoglobin (6 μM) was added to 1.5 mL of a solution containing cytochrome *b*₅ (6 μM) in the same buffer. The heme-transfer reaction was monitored spectrophotometrically at 20 °C by following the increase in absorbance at 406 nm. The traces were analyzed using the Beckman program.

Protein Denaturation by Urea. Urea denaturation of the cytochromes was examined by the change of the Soret band of the UV-vis spectrum on a Hewlett-Packard 8452A diode array spectrophotometer. Denaturation analysis was performed on the oxidized sample at a protein concentration of approximately 6 mM in 100 μ M sodium phosphate (pH 7.0) at 26 °C. Protein denaturation in urea was analyzed using eq 1 (36):

$$-RT \ln[(A_H - A_{412})/(A_{412} - A_A)] = \Delta G_D^0 - m[\text{urea}] \quad (1)$$

where A_{412} is the total absorbance at 412 nm. The values A_H and A_A are characteristic of the holoprotein and apocytochrome *b*₅, respectively. [urea] is the concentration of urea. ΔG_D^0 is the free energy of denaturation in the pure buffer, and m is the slope of the straight line characteristic of denaturing titrations. The difference in free energy of heme dissociation between the wild type and mutant protein was estimated at the midpoint of heme dissociation.

$$\Delta(\Delta G_D^{50\%}) = \langle m \rangle ([\text{urea}]_{WT}^{50\%} - [\text{urea}]_{mutant}^{50\%}) \quad (2)$$

where $[\text{urea}]^{50\%}$ are the values for the midpoints of heme dissociation for the wild-type and mutant proteins and $\langle m \rangle$ is the average of m for the wild-type and mutant proteins.

The denaturation rate of cytochrome *b*₅ (6 μ M) was studied under different concentrations of urea (100 mM sodium phosphate, pH 7.0) at 23 °C. The free energy of the activation of heme dissociation can be calculated using eq 3 (37–38):

$$\Delta G_D^\ddagger = -RT \ln(hk/k_B T) \quad (3)$$

where R is the gas constant, T is the absolute temperature, h is the Planck constant, k_B is the Boltzman constant, and k is the experimental rate constant of heme dissociation. The free energy of activation of heme dissociation, $\Delta G_D^{0\ddagger}$, at zero concentration of urea was estimated by linear extrapolation assuming that the linear dependence of ΔG_D^\ddagger on urea concentration and fits eq 4 (38):

$$\Delta G_D^\ddagger = \Delta G_D^{0\ddagger} - m_D^\ddagger [\text{urea}] \quad (4)$$

Electrochemical Measurements. Electrochemical experiments were performed using a PAR M273 potentiostat-galvanostat (PAR Princeton, NJ) which was interfaced to an IBM computer, controlled by PAR M270 software, and coupled with a Hewlett-Packard color photographer. A non-isothermal electrochemical cell, which consisted of a conventional two-compartment glass cell, was employed for the electrochemical measurements (39). The working electrode (WE) half-cell has a small volume sample ($V \sim 0.5$ mL) and is encased in a water jacket. The working electrode is a 2 mm diameter gold disk electrode, with a platinum wire coil as a counter electrode. Another half-cell with the Ag/AgCl (3 M KCl) reference electrode was physically isolated from the thermostated region of the WE half-cell by a salt bridge and kept at room temperature. The temperature of the working electrode half-cell was controlled to ± 0.2 °C by a circulating water bath (NESLAB, RTE-5B, Osaka, Japan). The temperature dependence of the formal reduction potential in this work was determined from 10.8 to 41.8 °C. Before

each measurement, the gold electrode was polished with 0.075 mm alumina, washed with twice-distilled water, ultrasonicated to remove adhesive alumina, and then thoroughly washed again. Afterward, the electrode cycled between +1.2 V and –0.6 V versus a Ag/AgCl electrode (+0.197 V vs NHE, 25 °C) repeatedly in 1 mM, pH 7.0 Hepes buffer solution containing 10 mM KCl, until the typical steady pattern of a clean gold surface was obtained. The modification with cysteine was completed by dipping the working electrode in 10 mM cysteine for 15 min and rinsing with twice-distilled water. Then the washed electrode was immersed immediately in the protein solution. Each working electrode was used for only one experiment.

Cyclic voltammetric experiments were carried out under anaerobic conditions by bubbling anaerobic nitrogen gas into the solution for 20 min. During the measurement, a stream of humidified nitrogen flowed across the surface of the solution. All the experiments were repeated more than five times. The values of half-wave potentials, which can be related to the formal reduction potentials, calculated by the equation $(E_{pa} + E_{pc})/2$ (where E_{pa} and E_{pc} are anodic and cathodic peak potentials, respectively), were found to be reproducible within ± 3 mV. All the potentials reported in this paper are referenced to NHE unless specifically stated.

RESULTS

Heme Dissociation of Cytochrome *b*₅ and Its Mutants upon Heating. As the temperature increased, the intensity of absorbance at 412 nm decreased; meanwhile when the temperature was higher than 80 °C, the absorbance peak shifted to 390 nm as shown in Figure 1. An isobestic point in the spectra upon heating indicates that the heme dissociation can be described as a two-state process. So the equilibrium constant and the free energy of heme dissociation can be calculated according to the following equations:

$$K_D = (A_H - A_{412})/(A_{412} - A_A) \quad (5)$$

$$\Delta G = -RT \ln K_D \quad (6)$$

where the A_{412} represents the absorbance at 412 nm of the protein solutions and A_H and A_A represent the protein absorbance at 25 °C (holo-protein) and 80 °C (apo-protein), respectively. The ΔG at given temperature can be calculated by eq 6. The ΔH and ΔS were obtained by curve fitting of the $\Delta G = \Delta H - T\Delta S$ equation. When the molar fraction of the holo-protein equals that of the apo-protein, that is, $f_A = f_H$, $\Delta G_D = 0$ and the transition temperature can be obtained according to $T_m = \Delta H_m/\Delta S_m$. The difference of free energy of thermal stability between the wild-type and the mutant proteins is described as:

$$\Delta(\Delta G_D) = \langle \Delta S_m \rangle [T_m(\text{mutant}) - T_m(\text{WT})] \quad (7)$$

where $\langle \Delta S_m \rangle$ is the average of ΔS_m of the wild-type and the mutant proteins. The thermodynamic parameters of these proteins upon heating are listed in Table 1. From the results it is shown that mutation at the surface residue of cytochrome *b*₅ did not significantly alter the thermostability of the proteins.

Heme Dissociation of Cytochrome *b*₅ in the Presence of Urea. The dissociation of heme from the protein in the

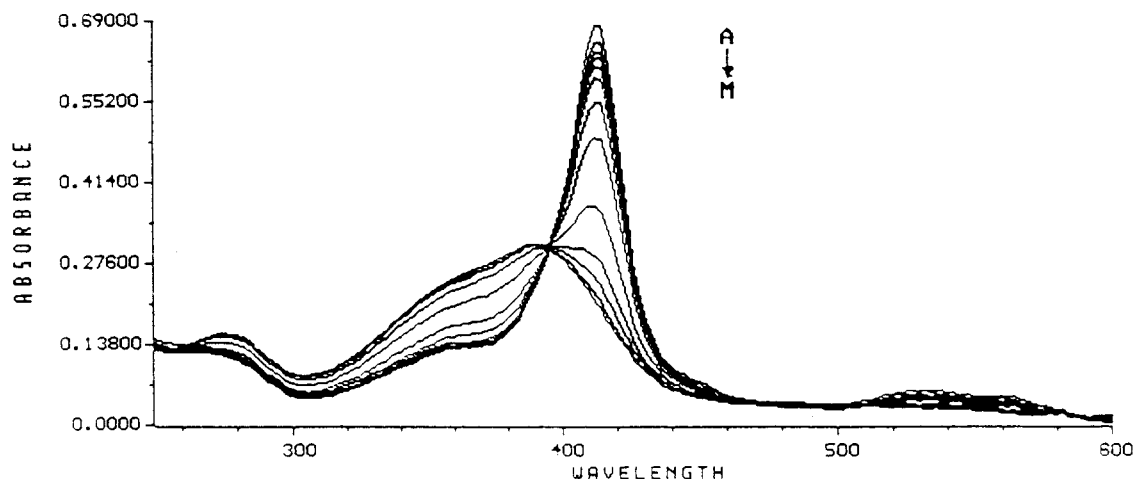


FIGURE 1: UV-vis spectra of cytochrome *b*₅ E44/56A upon heating. The concentration of protein is $\sim 6 \mu\text{M}$ in phosphate (100 mM, pH 7.0). Temperature: (A) 25.0, (B) 46.0, (C) 56.0, (D) 59.8, (E) 63.0, (F) 64.9, (G) 66.0, (H) 67.1, (I) 69.0, (J) 71.0, (K) 73.0, (L) 76.0, (M) 80.7 °C.

Table 1: The Thermodynamic Parameters of Cytochrome *b*₅ and Its Mutants upon Heating^a

	Cyt <i>b</i> ₅	Cyt <i>b</i> ₅ E44A	Cyt <i>b</i> ₅ E56A	Cyt <i>b</i> ₅ E44/56A
$\Delta(\Delta G_m)$ (kJ/mol)		-2.1	+4.6	+3.4
ΔH_m (kJ/mol)	449.8	446.0	463.6	478.7
ΔS_m (kJ/mol)	1.3	1.3	1.3	1.3
T_m (°C)	67.5	67.1	68.3	68.1

^a Phosphate buffer (100 mM, pH 7.0).

presence of urea was considered to be a two-state mechanism. This is verified by the existence of an isobestic point at 399 nm. The intensity of the Soret band of the wild-type and the mutant cytochrome *b*₅ at 412 nm decreases with increasing concentrations of urea, and the absorbance shifts to 400 nm (Figure 2a,b). When the Glu44 and Glu56 mutated to alanine, the urea concentration at the midpoint of heme dissociation, $[\text{urea}]_{1/2}$, increased and the difference in free energy between the wild-type and mutant protein at the midpoint of heme dissociation, $\Delta(\Delta G_D^{50\%})$, decreased (Table 2). These indicate that the order of stability of wild-type cytochrome *b*₅ and its mutants is as follows: WT < E44A < E56A < E44/56A.

The kinetics of the heme dissociation reaction of cytochrome *b*₅ in the presence of urea is a first-order reaction. The rate constants of heme dissociation increase with the increase in urea concentration, and the free energy of activation decreases with the increase in urea concentration (Figure 3). The free energies of activation of the heme dissociation for the wild type and for mutants E44A, E56A, and E44/56A of cytochrome *b*₅ are 98.28 ± 1.38 , 96.11 ± 1.51 , 96.23 ± 1.09 , and 96.02 ± 1.05 kJ/mol, respectively, when extrapolating to 0 concentration of urea. The free energies of activation of all mutants are almost the same. All of them decrease by 2.09 kJ/mol compared to that of the wild-type protein.

Solution pH Effect on the Stability of Cytochrome *b*₅ and Its Mutants. The spectra of protein solutions at different pH's are shown in Figure 4. The Soret band of the protein decreases with the increase of the acidity and shifts to 370 nm at pH = 2.0. Obviously, it is different from the case upon heating or in the presence of urea: no isobestic point existed in the spectra, indicating that it is not a simple two-

state process which is mainly related to the heme dissociation. The protein suffered extensive conformational changes by destroying the coordination bonding, hydrogen bonding, salt bridge, and so on. The middle point of acidic denaturation of cytochrome *b*₅ and its mutants occurs at approximately pH 4.0. Among these proteins no big difference is observed.

Heme-Transfer Reactions between Cytochrome *b*₅ and Apo-myoglobin. By using apo-myoglobin as a trap, the rate constants and activation free energy of the spontaneous dissociation of heme from cytochrome *b*₅ or its mutants E44A, E56A, and E44/56A were determined under non-denaturing conditions. It is shown in Figure 5. In Figure 5a, the Soret band shifts from 412 to 410 nm after mixing Cyt *b*₅ with apo-Mb and also the intensity increases; both indicate that the heme b is transferred from the Cyt *b*₅ to apo-Mb. The heme-transfer reaction consists of two steps: the first step is to release the heme from cytochrome *b*₅; the second one is to connect apo-myoglobin with the heme b. Since the whole reaction is slow and the second step is very fast ($k = 5.8 \times 10^5 \text{ M}^{-1} \text{ s}^{-1}$) (40), the first step is the rate-determining step for the whole reaction and the heme-transfer reaction can be treated as a first-order reaction. The rate constants of the heme transfer from wild-type cytochrome *b*₅ or mutant E44A, E56A, or E44/56A to apo-myoglobin and the corresponding activation energies of the heme dissociation calculated from the Figure 5b data are listed in Table 3. Obviously, mutation of Glu44 or Glu56 to alanine led to a decrease of heme-transfer rates. The rate ratio is 100(WT):93(E44A):64(E56A):51(E44/56A). The rate of Cyt *b*₅ E44/56A is almost half of that of the wild-type protein. It gives a good indication that the mutation of the hydrophilic residues (Glu) sited at helices near the heme to hydrophobic residues (Ala) leads to a more compact heme pocket.

The Temperature Dependence of Reduction Potentials of Five Individual Proteins. The cyclic voltammograms of cytochrome *c*, the wild type, and the E44/56A mutant of cytochrome *b*₅ at different temperatures are shown in Figure 6. At varied temperatures, slightly different voltammetric behavior is noted. For cytochrome *c*, the peak currents increase with the increase in temperature and also the peak currents of cytochrome *c* are higher than that of cytochrome

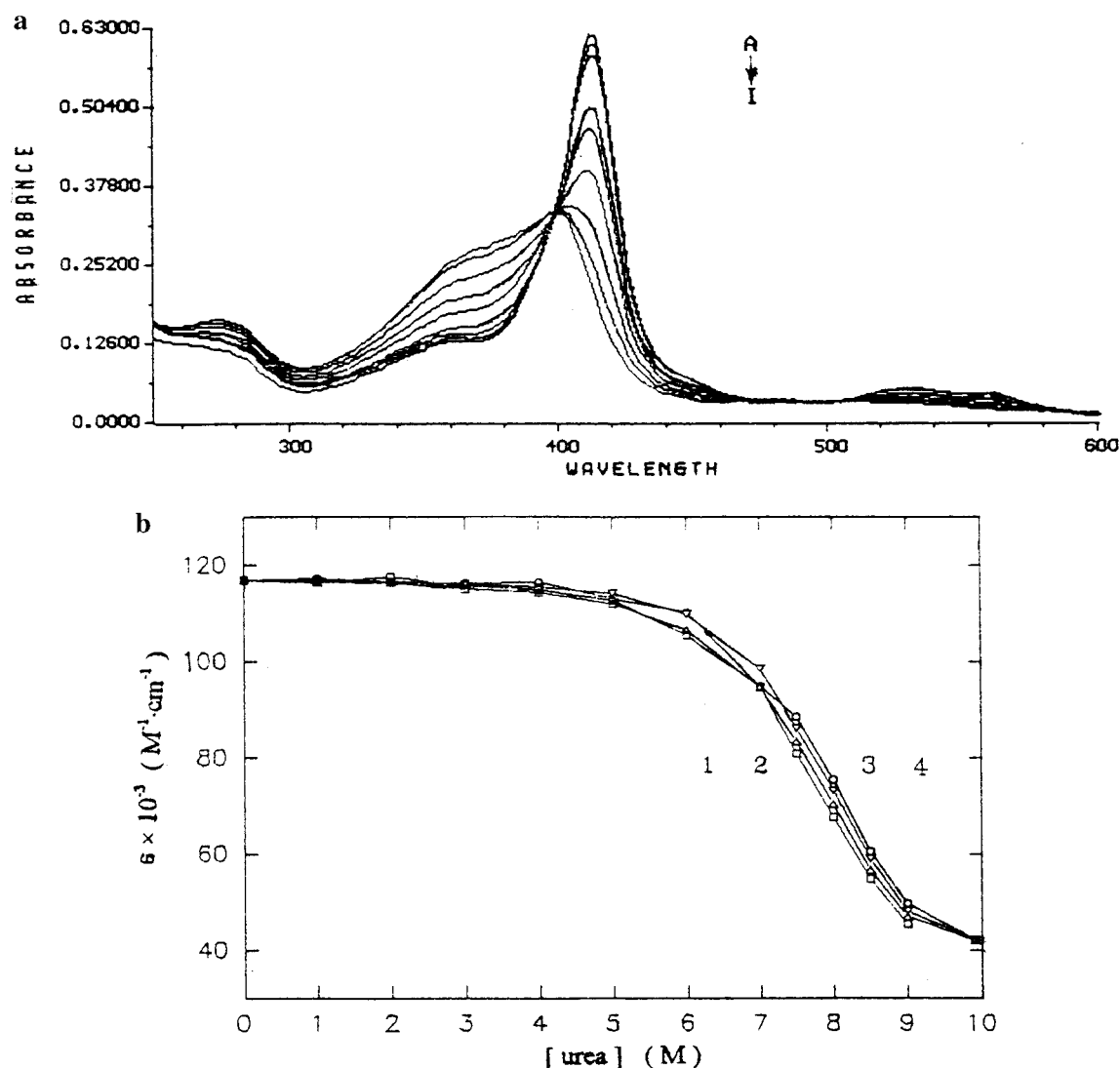


FIGURE 2: (a) UV-vis spectra of cytochrome *b*₅ E44/56A at different urea concentrations: (A) 0.0, (B) 5.0, (C) 6.0, (D) 7.0, (E) 7.5, (F) 8.0, (G) 8.5, (H) 9.0, (I) 9.9 M. (b) Extinction coefficients of cytochrome *b*₅ wild type (1), E44A (2), E56A (3), and E44/56A (4) as a function of the urea concentration.

Table 2: Values of [urea]_{1/2} and $\Delta(\Delta G_D^{50\%})$ for the Global Unfolding Equilibrium in Urea Solutions of Cytochrome *b*₅ and Its Mutants^a

cytochrome	wild type	E44A	E56A	E44/56A
[urea] _{1/2} (M)	7.77 ± 0.01	7.83 ± 0.02	8.00 ± 0.02	8.06 ± 0.03
$\Delta(\Delta G_D^{50\%})$ (kJ/mol)		-0.21	-0.75	-0.96

^a Phosphate buffer (100 mM, pH 7.0), 26 °C. The values are the average of three measurements.

*b*₅ at the same protein concentration at all temperatures. The same situations are observed for E44A and E56A mutants of cytochrome *b*₅. These observations imply that there are different protein/electrode properties for positively charged cytochrome *c* and negatively charged cytochrome *b*₅ or its mutants at varied temperatures. Indeed, we have confirmed (25) that, in the absence of Mg²⁺ ion, the positively charged cytochrome *c* can directly display a reversible voltammetric behavior by electrostatic interaction between its lysine residues and the negatively charged surface of the electrode. However, the electrochemical response of negatively charged cytochrome *b*₅ is stimulated only in the presence of Mg²⁺ ion. Therefore, we suggested in that paper that for cytochrome *b*₅ there is a Mg²⁺ ion bridging the protein to the electrode. The binding of Cyt *b*₅/Mg²⁺/electrode is also possibly affected by temperature variation here. Meanwhile,

it is interesting to note that the peak-to-peak separation, ΔE_p , for five individual proteins, decreases as the temperature increases (e.g., the $\Delta(\Delta E_p)$ between 10.8 and 41.8 °C for cytochrome *c* is 29 mV and for the wild-type cytochrome *b*₅ is 16 mV). This suggests that the linear diffusion mechanism dominates the electrochemical process more and more as the temperature increases (Table 4). From the peak shape changes of the cyclic voltammograms, especially for the cytochrome *c*, it is evident that an almost perfect peak shape voltammogram develops as the temperature increases. The changes of electrochemical kinetics can be attributed to the de-absorption of the protein molecules on the electrode leading to the increase of the electroactive sites at the surface of the modified electrode (25, 41–42) and the increase of the diffusion coefficient of the electroactive species at higher temperature. Furthermore, we observed the negative shifts

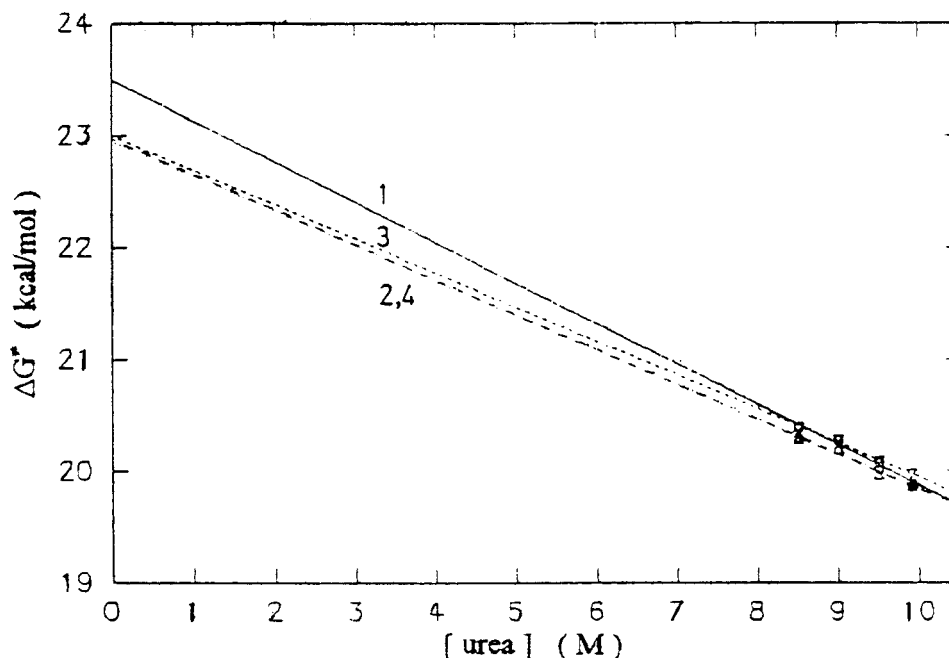


FIGURE 3: Free energy of activation of heme dissociation as a function of the urea concentrations. Cytochrome b_5 wild type (1), E44A (2), E56A (3), and E44/56A (4). The correlation coefficients for all fittings are 0.997.

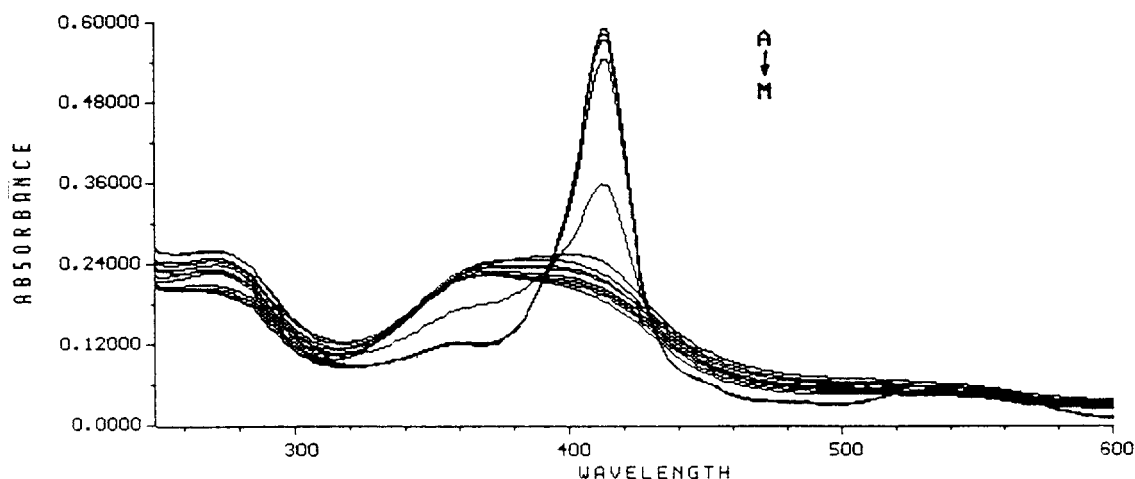


FIGURE 4: UV-vis spectra of cytochrome b_5 E44/56A at different pH values: (A) 5.67, (B) 5.21, (C) 4.70, (D) 4.36, (E) 4.01, (F) 3.68, (G) 3.36, (H) 3.19, (I) 3.04, (J) 2.82, (K) 2.66, (L) 2.51, (M) 2.26.

of both the cathodic and the anodic peaks for cytochrome c , cytochrome b_5 , and its three mutants with increasing temperature, resulting in the decrease of the formal reduction potential at higher temperature (Table 4). The negative shifts in formal reduction potentials indicate the relative stability of the oxidized and reduced forms. For cytochrome c , the shifts of the thermodynamic equilibrium at variable temperatures could be attributed to gradual changes in the conformation with temperature. Moore et al. (43) conducted a NMR study of the temperature effect on the conformation of cytochrome c ; they found that, as the temperature increases, the crevice around the solvent-exposed heme edge opens and allows greater exposure of the heme to the solvent, thus stabilizing the positively charged heme group of ferricytochrome c . The same mechanism should also account for the case of cytochrome b_5 .

Indeed, Taniguchi and co-workers (44–45) studied the influence of temperature, electrolyte composition, and pH upon the reduction potential of horse heart cytochrome c

using a gold electrode “pre-dip modified” with bis(4-pyridyl) disulfide over the range 0–55 °C at pH 6, 7, and 8. Since they have not observed significant change in the structure of the promoter/electrode interface as monitored by surface-enhanced Raman resonance spectroscopy, we conclude that the different temperature dependence of the formal reduction potentials and the entropy changes should be mainly associated with both the native structure of the proteins and the mode of interaction between the proteins and the electrode. On the basis of the results obtained from the denaturation upon heating, we suggest that the negative shifts in formal reduction potentials of cytochrome b_5 and its mutants with the increase in temperature should be attributed to the conformational changes, just like that of cytochrome c mentioned previously. In summary, the temperature shifted the redox equilibrium for both cytochrome c and cytochrome b_5 or its mutants by changing their framework structures. Noteworthy is that the E'^{25} (the formal reduction potential at 25 °C) of cytochrome b_5 and its mutants, obtained from

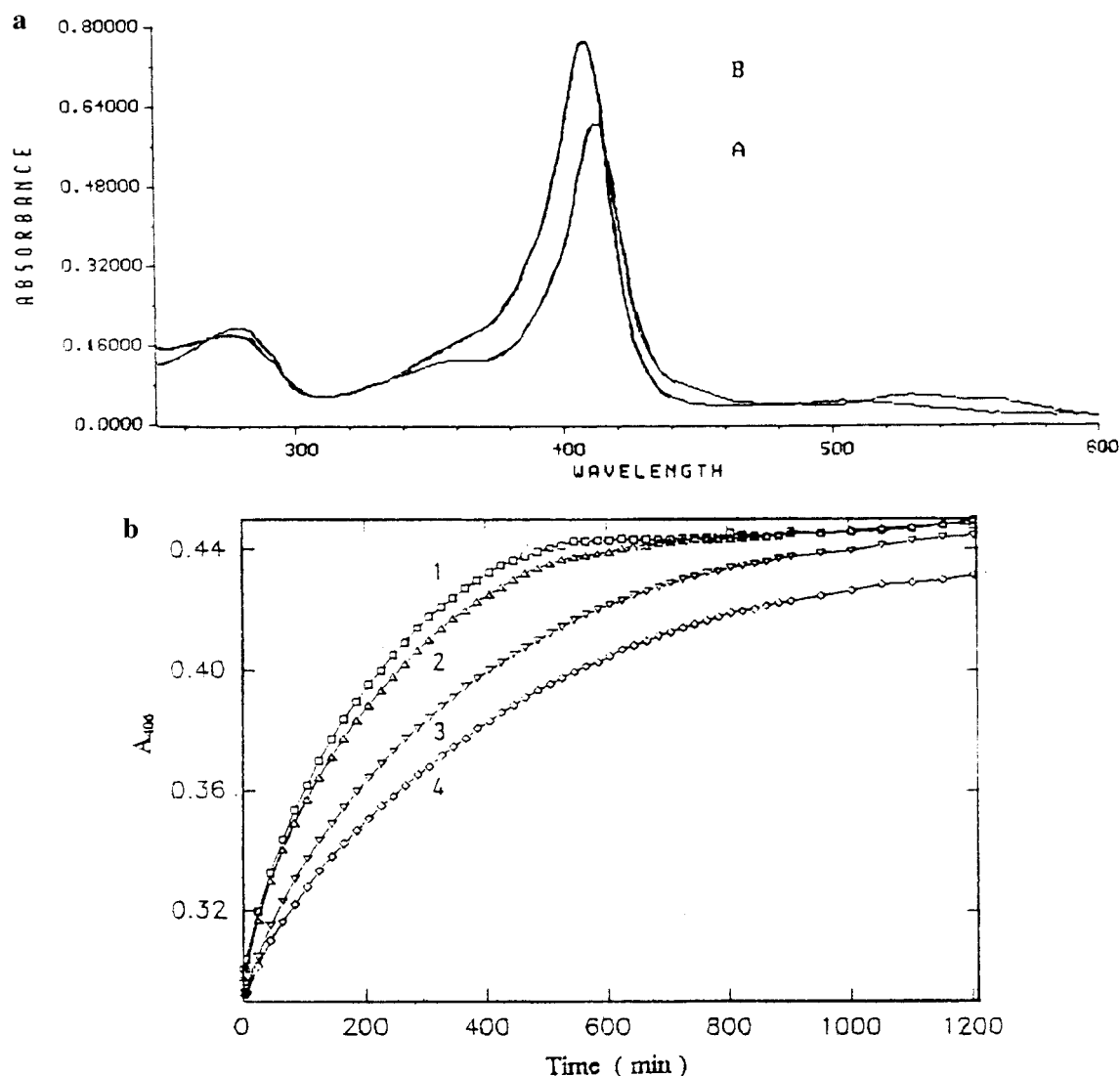


FIGURE 5: (a) UV-vis spectra of heme-transfer reaction between cytochromes and apo-myoglobin (A) before mixing and (B) after mixing for 25 h. (b) Kinetic traces for heme-transfer reaction between apo-myoglobin and (1) wild-type Cyt *b*₅; (2) Cyt *b*₅ E44A; (3) Cyt *b*₅ E56A; and (4) Cyt *b*₅ E44/56A.

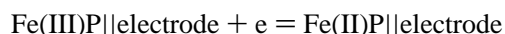
Table 3: The Kinetic Parameters of the Heme-Transfer Reactions between Cytochrome *b*₅, Its Mutants, and Apo-myoglobin^a

cytochrome	wild type	E44A	E56A	E44/56A
<i>k</i> (h ⁻¹)	0.28	0.26	0.18	0.14
ΔG_D^\ddagger (kJ/mol)	95.8	95.8	97.1	97.5

^a Phosphate buffer (1 mM, pH 6.8), 20 °C.

the plots of E° vs T , has similar values (Table 5), indicating that the three mutant proteins have redox properties similar to those of wild-type cytochrome *b*₅ and the mutation at residues E44 and E56 did not perturb the heme environment of cytochrome *b*₅ significantly.

Entropy Effects for Five Individual Protein Systems. It has been suggested that the heterogeneous electron-transfer reaction of the cytochromes at the electrode can be associated with the redox couple as follows (46):



(where P represents the protein part, except the prosthetic group, heme). Therefore, from the absolute entropy difference of the reduction state and the oxidation state, we can

obtain the reaction center entropy changes, $\Delta S^\circ_{\text{rc}}$. Weaver et al. (39) have described the entropy behaviors of some metal redox couples in solution in detail. In the non-isothermal cell, the reaction center entropy changes, $\Delta S^\circ_{\text{rc}}$, can be obtained from the temperature coefficient, dE°/dT , according to eq 8:

$$\Delta S^\circ_{\text{rc}} = nF(dE^\circ/dT) = S^\circ_{\text{red}} - S^\circ_{\text{ox}} \quad (8)$$

where n is the number of electrons transferred, F is the Faraday constant, E° is the formal reduction potential, and T is the temperature of the redox couple of interest. A linear regression fit of E° versus temperature data is used to calculate the formal reduction potential at 25 °C, E°_{25} .

Figure 7 shows the dependence of the formal reduction potential upon temperature obtained from Figure 6. Linearity is observed from 10.8 to 41.8 °C for either cytochrome *c* or cytochrome *b*₅ and its mutants. From the slopes of the plots of E° vs T , the temperature coefficients, dE°/dT , were obtained and the values for different protein systems were calculated. These results are summarized in Table 5. Noteworthy is that all proteins studied here exhibit essentially negative entropy changes on electron-transfer reactions, but

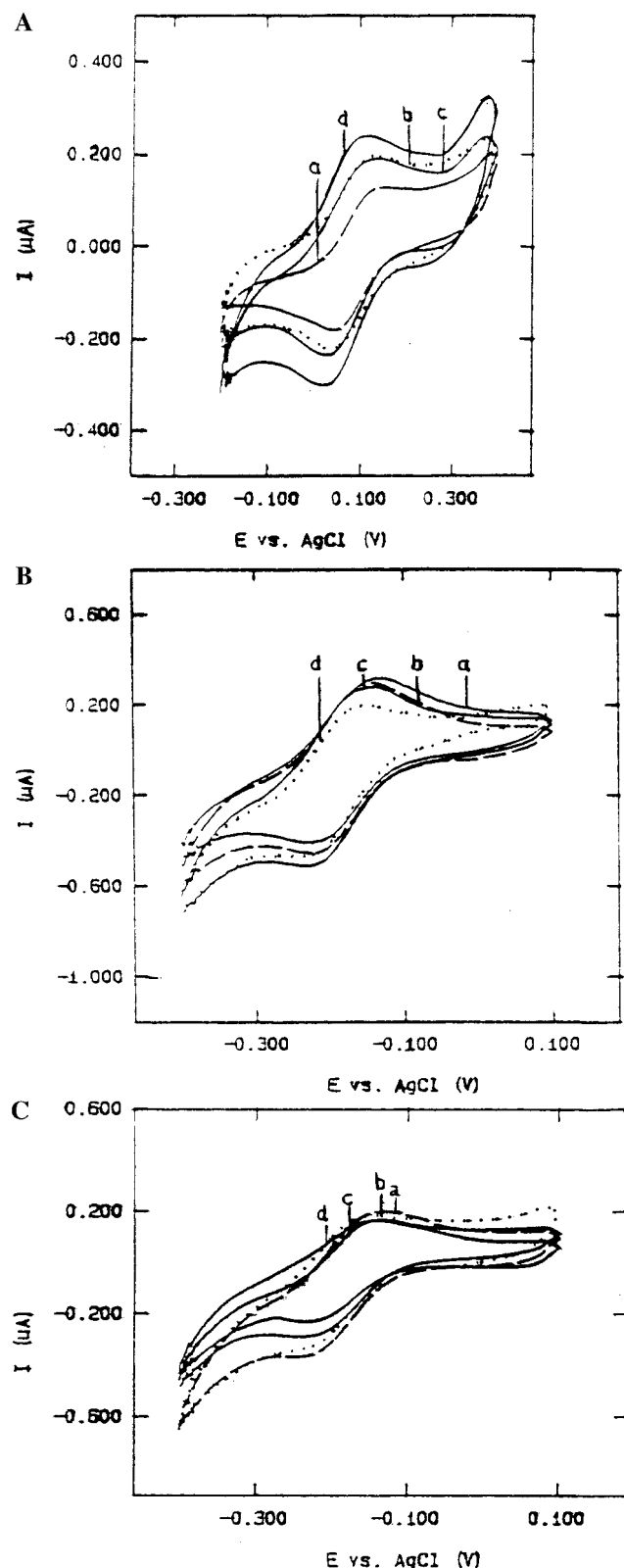


FIGURE 6: The typical cyclic voltammograms of (A) cytochrome *c*, (B) wild type of cytochrome *b*₅, and (C) E44/56A of cytochrome *b*₅ at variation temperatures: (a) 10.8, (b) 20.6, (c) 30.6, (d) 41.8 °C. Experimental conditions: pH 7.0, 1 mM Hepes buffer solutions containing 0.2 mM proteins, 20 mM KCl, and 4 mM MgCl₂. Scan rate: 50 mV/s.

the negative entropy changes are very different in magnitude.

It is well-known that cytochrome *c* is a positively charged protein (ca. +7 at pH 7.0), and cytochrome *b*₅ is a negatively

Table 4: The Temperature Dependence of Formal Reduction Potentials and the Peak Separations of Five Proteins Alone^a

<i>T</i> (°C)	Cyt <i>c</i>		Cyt <i>b</i> ₅		E44A		E56A		E44/56A	
	<i>E</i> _{1/2}	Δ <i>E</i> _p	<i>E</i> _{1/2}	Δ <i>E</i> _p	<i>E</i> _{1/2}	Δ <i>E</i> _p	<i>E</i> _{1/2}	Δ <i>E</i> _p	<i>E</i> _{1/2}	Δ <i>E</i> _p
10.8	292	110	27.5	97	12.2	94	17.8	97	10.5	93
20.6	284	93	16.6	85	7.5	89	6.0	100	7.2	84
23.0	280	79	9.2	76	6.0	83	4.8	90	5.2	84
30.6	272	87	4.6	85	3.4	84	1.0	98	4.6	81
41.8	256	81	-4.0	81	2.1	76	-5.8	90	0.4	74

^a The *E*_{1/2} and Δ*E*_p are in mV. The values of *E*_{1/2} and Δ*E*_p at this temperature were determined when the protein solutions were prepared and equilibrated for 20 min. All results are the average from five experiments. Protein concentrations are 0.2 mM in pH 7.0, 1 mM Hepes solutions containing 20 mM KCl and 4 mM MgCl₂.

charged protein (ca. -8 at pH 7.0). It was concluded that "the Δ*S*_{rc} values for the electron-transfer metalloproteins are all negative" (28); that is in contrast with those found in the simple inorganic complexes of iron [e.g., considering the following Δ*S*_{rc} values: Fe(H₂O)₆^{3+/2+}, +43 eu, (39) Fe(CN)₆^{3-/4-}, -49 eu (47)]. In connection to our studies it is true that both proteins exhibit negative entropy changes. For cytochrome *c*, the Δ*S*_{rc} is -118.7 J/mol·K. The entropy changes, Δ*S*_{rc}, for different cytochrome *b*₅ species are very different in magnitude (Table 5) even though under these conditions no remarkable differences were observed in the formal reduction potentials among these cytochrome *b*₅ variants. The Δ*S*_{rc} values are -95.3, -37.2, -67.7, and -31.3 J/mol·K for the wild type and for E44A, E56A, and E44/56A of cytochrome *b*₅, respectively. Obviously, their Δ*S*_{rc} values do not correlate with the overall charges on the proteins. Our experimental results probably demonstrate that for the macromolecule complexes, such as the redox metalloproteins studied here, the important contributions to the electron-transfer reaction entropy changes should mainly come from the changes in their framework structures and the charge-induced solvent molecule rearrangements.

The Temperature Dependence of the Formal Reduction Potential of Individual Proteins in 1:1 Protein Complexes.

As mentioned, the main aim of our present work is to reveal whether the Glu44 or Glu56 is involved in the formation of the cytochrome *b*₅/cytochrome *c* complex. To investigate the role that the carboxylate groups of E44 and E56 of cytochrome *b*₅ played in the interaction with cytochrome *c*, we studied the 1:1 protein/protein systems composed of cytochrome *c* and cytochrome *b*₅ or its three mutants under the same experimental conditions. We selected the gold electrode modified with cysteine to study the cyclic voltammetric behavior, since under this condition, we can obtain both of the electrochemical responses contributed by the two individual proteins simultaneously. The temperature dependence of 1:1 protein/protein complex systems of Cyt *c*/Cyt *b*₅, Cyt *c*/Cyt *b*₅ E44A, Cyt *c*/Cyt *b*₅ E56A, and Cyt *c*/Cyt *b*₅ E44/56A was studied, and the cyclic voltammetric diagram of Cyt *c*/Cyt *b*₅ complex at different temperature is shown in Figure 8. Obviously, cytochrome *c* or cytochrome *b*₅ in 1:1 protein complexes displays different voltammetric behavior from that in the individual proteins alone (25). The negative potential shifts with increase in temperature for cytochrome *c* and cytochrome *b*₅ are observed; however, they have different magnitudes compared with those measured when each protein is alone. Table 6 summarizes the formal

Table 5: Thermodynamic Parameters for Proteins Alone and in 1:1 Protein/Protein Complexes^a

species	$E^{\circ\prime}_{25}$ (mV)	ΔS°_{rc} (J/mol·K)	ΔS° (J/mol·K)	ΔH° (kJ/mol)	ΔG° (kJ/mol)
Cyt <i>c</i> (alone)	+278	-118.7	-184.0	-81.4	-26.8
Cyt <i>c</i> (in <i>c/b₅</i>)	+271	-51.8	-117.0	-61.0	-26.2
Cyt <i>c</i> (in <i>c/E44A</i>)	+269	-79.8	-145.0	-69.2	-26.0
Cyt <i>c</i> (in <i>c/E56A</i>)	+271	-56.1	-121.3	-62.3	-26.2
Cyt <i>c</i> (in <i>c/E44/56A</i>)	+272	-110.0	-175.2	-78.4	-26.2
Cyt <i>b₅</i> (alone)	+9	-95.3	-160.5	-48.7	-0.9
Cyt <i>b₅</i> (in <i>c/b₅</i>)	+17	-63.4	-128.6	-40.0	-1.6
E44A (alone)	+5	-37.2	-102.4	-31.0	-0.5
E44A (in <i>c/E44A</i>)	+4	-53.3	-118.5	-35.7	-0.4
E56A (alone)	+6	-67.7	-133.0	-40.2	-0.6
E56A (in <i>c/E56A</i>)	+9	-50.3	-115.5	-35.3	-0.9
E44/56A (alone)	+6	-31.3	-96.5	-29.3	-0.6
E44/56A (in <i>c/E44/56A</i>)	+7	-54.4	-119.6	-36.3	-0.7

^a All ΔS°_{rc} values reported were the averages obtained from the linear regression of five $E^{\circ\prime}$ vs T data sets at 50 mV/s, and the values of ΔS° and ΔH° were calculated according to eqs 9 and 10 (for details see text). Experimental conditions: protein concentrations are 0.2 mM in pH 7.0, 1 mM Hepes solutions containing 20 mM KCl and 4 mM Mg²⁺ ion. The value for $E^{\circ\prime}$ at 25 °C was extrapolated from the experimentally determined $dE^{\circ\prime}/dT$.

reduction potentials of each protein individually involved in four protein/protein complexes at different temperatures. We observed not only the different changes in the formal reduction potentials of cytochrome *c* in four complexes but also the striking differences in the potentials of wild-type cytochrome *b₅* and its three mutants in protein complexes compared with those of the individual proteins alone. Since we performed the experiments on the protein/protein systems under the same conditions as on the individual protein, that is, the protein concentration, the cation concentration, the solvent environment, and the ionic strength were the same, the discrepancy between protein/protein systems and the individual protein on the temperature dependence of formal reduction potential can be considered as the reflection of their rather specifically mutual interactions between the cytochrome *c* and cytochrome *b₅* or its three mutants.

The Entropy Effects in 1:1 Cytochrome *c*/Cytochrome *b₅* Complex Systems. To elucidate the mutual interaction in detail, from the plots of $E^{\circ\prime}$ vs T (Figure 7), the entropy changes of individual proteins in four protein complexes were calculated. Table 5 summarizes the experimental results for all 1:1 protein/protein complex systems studied here. All proteins in complexes exhibited negative entropy changes too. In contrast to the small changes in the formal reduction potentials and the free energies, we observed marked differences in the entropy changes. The entropy changes of cytochrome *c* are -51.8, -79.8, -56.1, and -110.0 J/mol·K in the 1:1 protein/protein complexes formed with the wild type and with E44A, E56A, and E44/56A of cytochrome *b₅*, respectively. The differences between these entropy changes and those obtained when cytochrome *c* is alone (at that time the ΔS°_{rc} is -118.7 J/mol·K) are +66.9, +38.9, +62.6, and +8.7 J/mol·K, respectively. These results, no doubt, reflect the differences in the mutual interaction of cytochrome *c* with different cytochrome *b₅* species.

DISCUSSION

The Stability Comparison between the Wild-Type Cytochrome *b₅* and the Mutant Proteins. The [urea]_{1/2}, the $\Delta(\Delta G_D^{50\%})$, and the rate constants of heme-transfer reaction can be used as indications of structural stability of these proteins. When Glu44 and Glu56, which are on the surface of cytochrome *b₅* and surround the open side of the

hydrophobic pocket of the heme, were mutated to alanine, the stability of the protein increased slightly. According to the [urea]_{1/2} and $\Delta(\Delta G_D^{50\%})$, the order of stability is the following: cytochrome *b₅* (WT) > E44A > E56A > E44/56A. The same order is obtained from the study of the heme-transfer reactions between cytochrome *b₅* and apo-myoglobin.

Both the Glu44 and the Glu56 locate at the amino terminal of two helices in cytochrome *b₅* (Gly42-Gln49 and Ala54-Val61). The placement of acidic residues at the amino termini of helices or the placement of basic residues at the carboxylate termini of helices will generally increase the stability of the protein (48–49). So, the stability of cytochrome *b₅* should be decreased with the mutation of Glu44 and Glu56 to alanine. To our surprise, a slight increase in the stability of mutants E44A, E56A, and E44/56A toward heme-transfer reaction and denaturation by urea is evident. One very possible reason is that the Glu44 and Glu56 situate at two different hydrogen bond networks of cytochrome *b₅* as shown in Figure 9 (9, 50). In the Glu56 related hydrogen bond network the backbone carbonyl (amide-O) of Glu56 forms two hydrogen bonds with backbone amide hydrogen (amide-H) of Asp60 and Glu59, respectively, that are believed to stabilize the heme/protein complex (51). It is in the situation similar to that of Glu56 that the Glu44 is situated at another hydrogen bond network. In wild-type cytochrome *b₅*, the negatively charged side chains of Glu44 and Glu56 interact with water molecules and stick out into the solution. There are two forces to pull two pairs of helices from two sides of the heme through hydrogen bond networks. When the hydrophilic residues, glutamate, were changed to hydrophobic residues, alanine, some of hydrogen bonds disappeared and the balance of forces was altered, resulting in the heme being more tightly held by the two pairs of helices. Actually, a detailed NMR study did show that when the Glu44 and Glu56 were mutated into alanine, the chemical shifts of the backbone of these two helices moved. Even the whole overall structure of cytochrome *b₅* remained unaltered, the local conformational changes did occur at the two helices where the Glu44 and Glu56 situated (52–53). Meanwhile, comparing the hydrogen bond network at the Glu56 side with the network at the Glu44 side, there are more hydrogen bonds and the hydrogen bonds are arranged more compactly in the former network.

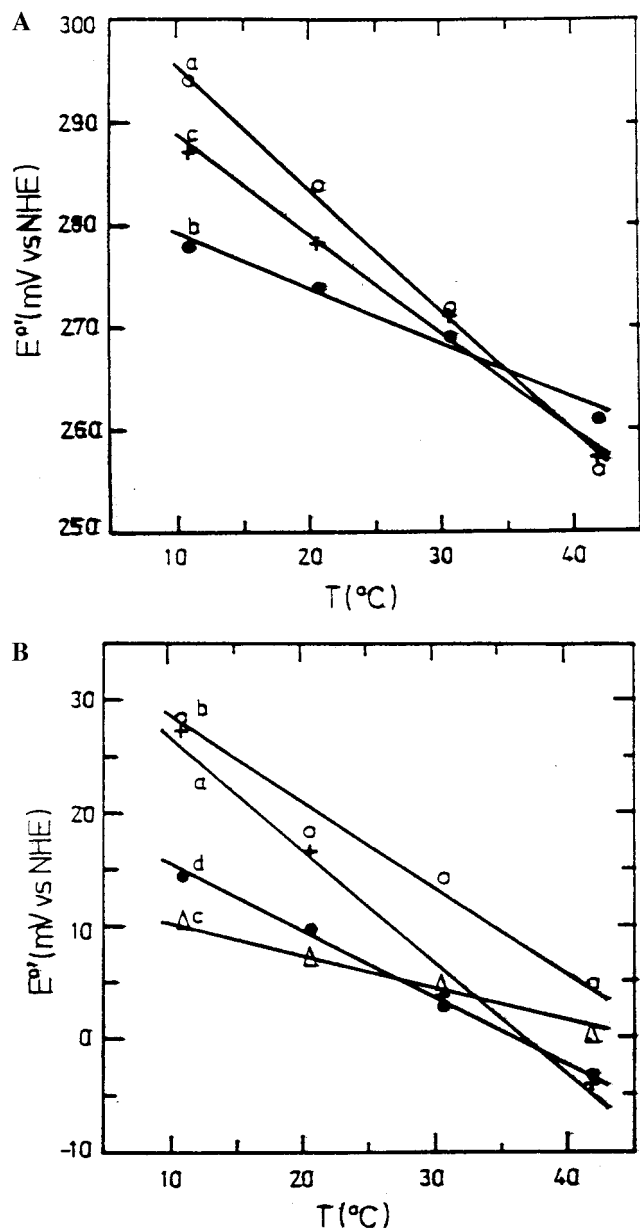


FIGURE 7: The typical dependence of the $E^{\circ'}$ values on the temperatures obtained from Figure 6. (A) cytochrome *c* alone (a), cytochrome *c* in Cyt *c*/Cyt *b*₅ (b), cytochrome *c* in Cyt *c*/Cyt *b*₅ E44/56A (c), (B) cytochrome *b*₅ alone (a), cytochrome *b*₅ in Cyt *c*/Cyt *b*₅ (b), E44/56A of cytochrome *b*₅ alone (c), E44/56A of cytochrome *b*₅ in Cyt *c*/Cyt *b*₅ E44/56A (d).

This makes the part of the protein molecule where the Glu44 is located more flexible than the part of the molecule where the Glu56 is located. Therefore, it is understandable that the influence of mutation at the Glu56 on the stability of cytochrome *b*₅ is bigger than at the Glu44. With the synergistic effect, the two-site mutant Cyt *b*₅ E44/56A is more stable than its single-site mutant E44A or E56A. It is claimed that the increasing stability of the protein in the mutation of cytochrome *b*₅ is comparatively rare (54); however in fact, the Cyt *b*₅ Phe35Tyr mutant obtained in this laboratory also shows a higher stability than the wild-type protein (55).

The Temperature Dependence of Formal Reduction Potentials and the Entropy Effects for Five Individual Proteins. From Table 4 it shows that when the temperature increases, the variation of the formal reduction potential is different in

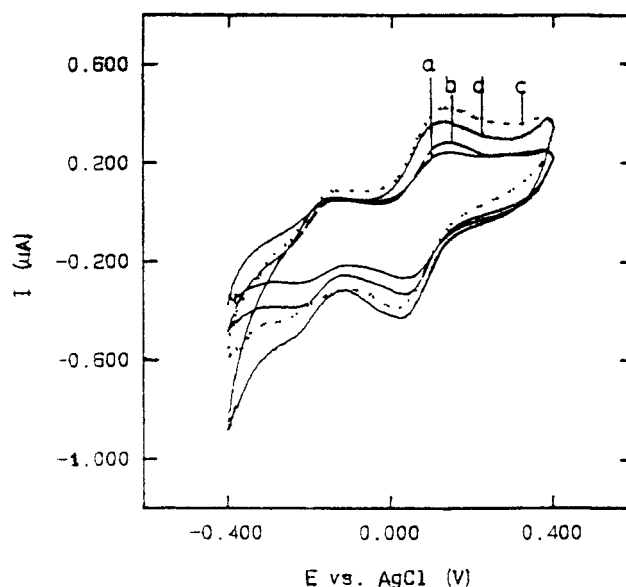


FIGURE 8: Cyclic voltammograms of 1:1 protein complex formed by 0.2 mM cytochrome *c* and wild type of cytochrome *b*₅ at variation temperatures: (a) 10.8, (b) 20.6, (c) 30.6, (d) 41.8 $^{\circ}\text{C}$. Experimental conditions: pH 7.0, 1 mM Hepes buffer solutions containing 20 mM KCl and 4 mM MgCl_2 . Scan rate: 50 mV/s.

magnitude for cytochrome *c*, cytochrome *b*₅, and its mutants. The negative shifts of formal reduction potential from 10.8 to 41.8 $^{\circ}\text{C}$ for cytochrome *c*, cytochrome *b*₅, and the E44A, the E56A, and the E44/56A of cytochrome *b*₅ are 36.0, 31.5, 10.1, 23.6, and 10.1 mV, respectively. Obviously, with the increase in temperature the oxidized states of these proteins are being stabilized. Compared with the wild-type cytochrome *b*₅, the mutants, especially these containing the E44A mutation showed small shifts in formal reduction potential, implying that the mutation at E44 made the protein more compact. It might suggest that, for the E44A-containing mutants, with the increase in temperature, less conformational change around the open side of the heme hydrophobic pocket is induced, resulting in less shift in formal reduction potentials. This is in good agreement with our thermal stability study on these proteins described in previous sections. In particular, it might further imply that although the mutagenesis on the surface residues did not alter the secondary and tertiary structures of cytochrome *b*₅ significantly (18), it did influence the redox behaviors of the wild type and its mutants in a different way by subtly disturbing the local structure.

Analyzing the reduction process, the contribution of entropy changes mainly comes from the following three sources: (1) the water solvation entropy on the protein surface; (2) as indicated in the protein interiors the water molecules are more highly ordered in the reduction state than in the oxidized state (21, 56): the number and the extent of the disorder in the interior water molecules inside the protein contribute to the entropy changes; (3) the protein itself becomes more rigid in the reduced state, contributing to the protein conformational entropy (21, 56). One thing that is worthy of further discussion is the main factors influencing the entropy behaviors of these proteins studied. As we know, cytochrome *b*₅ is a negatively charged protein with net charge -8 at pH 7.0, when the Glu44 or Glu56 is changed to Ala44 or Ala56, the net negative charges are -7 , -7 , and -6 for E44A, E56A, and E44/56A of cytochrome *b*₅, respectively.

Table 6: The Temperature Dependence of Reduction Potentials of both Cytochrome *c* and Cytochrome *b*₅ and Its Mutants in Their 1:1 Protein/Protein Complexes^a

<i>T</i> (°C)	Cyt <i>c</i> /Cyt <i>b</i> ₅				Cyt <i>c</i> /E44A				Cyt <i>c</i> /E56A				Cyt <i>c</i> /E44/56A			
	Cyt <i>c</i>		Cyt <i>b</i> ₅		Cyt <i>c</i>		Cyt <i>b</i> ₅		Cyt <i>c</i>		Cyt <i>b</i> ₅		Cyt <i>c</i>		Cyt <i>b</i> ₅	
	<i>E</i> _{1/2}	Δ <i>E</i> _p	<i>E</i> _{1/2}	Δ <i>E</i> _p	<i>E</i> _{1/2}	Δ <i>E</i> _p	<i>E</i> _{1/2}	Δ <i>E</i> _p	<i>E</i> _{1/2}	Δ <i>E</i> _p	<i>E</i> _{1/2}	Δ <i>E</i> _p	<i>E</i> _{1/2}	Δ <i>E</i> _p	<i>E</i> _{1/2}	Δ <i>E</i> _p
10.8	278	104	28.5	99	282	99	13.0	100	280	98	17.8	98	287	113	14.5	94
20.6	274	99	18.5	86	276	96	4.5	98	272	99	15.5	92	278	107	9.8	86
23.0	270	84	16.0	72	270	90	4.0	80	270	80	13.6	74	275	88	8.1	83
30.6	269	99	14.5	83	259	92	2.0	92	269	97	4.0	92	271	86	3.1	86
41.8	261	96	5.0	69	256	90	−5.2	84	261	97	−1.5	86	257	81	−3.0	81

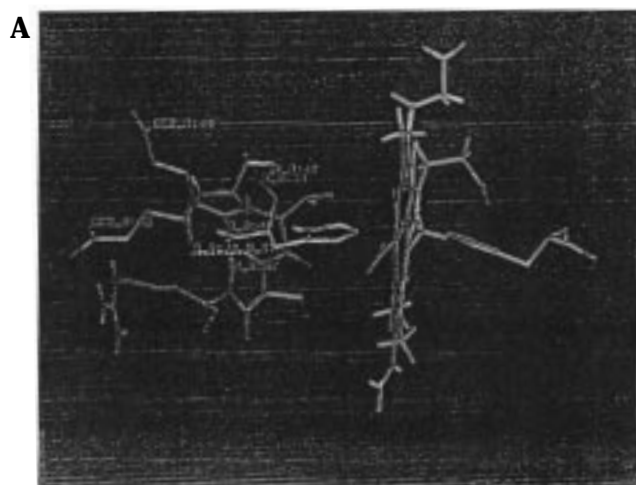
^a Both *E*_{1/2} and Δ*E*_p are in mV. The values of *E*_{1/2} and Δ*E*_p at this temperature were determined when the protein solutions were prepared and equilibrated for 20 min. All results are the average of five experiments. Protein concentrations are 0.2 mM in pH 7.0, 1 mM Hepes solutions containing 20 mM KCl and 4 mM MgCl₂.

Here, because the net charge changes upon reduction for all proteins are one unit, the removal of one (in the mutants of E44A or E56A mutant) or two negative charges (in the E44/56A mutant) from the protein surface would not bring about significant entropy effect. As we mentioned previously, one part of the protein molecule where the E44 is situated is more flexible than the other part of the protein where the E56 is situated. So, in comparison with wild-type cytochrome *b*₅, these mutants exhibit more rigid protein structures due to the decrease of the residue volume [Glu → Ala, about 64 Å³, (57)] and the increase of hydrophobicity. Therefore, we suggest that the main contribution to the negative entropy changes upon reduction is probably from the conformational change entropy. The larger negative entropy change of the wild-type cytochrome *b*₅ results from a larger conformational change of a more loose structure of the protein; the smaller entropy changes of E44A, E56A, and E44/56A of cytochrome *b*₅ should obviously attribute to their more compact and stable structures. Furthermore, we also observed that, in the single-protein systems, the Δ*S*_{rc} values of E44A and E44/56A of cytochrome *b*₅ are smaller than that of cytochrome *b*₅ E56A. It might imply that the mutation at site 44 brought about a larger influence on protein structure than at site 56, so their structural changes upon reduction become smaller than that of the E56A mutant, and this is in good agreement with our NMR study on cytochrome *b*₅ E44/56A (53). The Δ*S*_{rc} values for individual cytochrome *c* and cytochrome *b*₅ measured here are −118.7 and −95.3 J/mol·K, respectively, which are negative values larger than that reported elsewhere (58–60). We assume that this is because we determined the Δ*S*_{rc} at lower ionic strength; under these conditions the proteins experience larger variation in conformation.

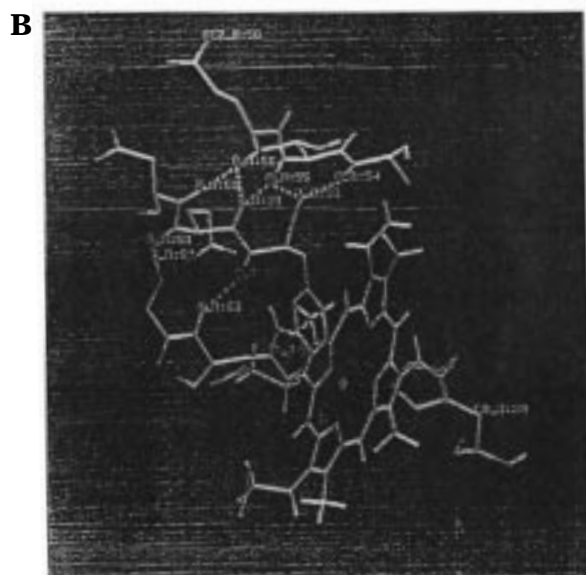
The Temperature Dependence of the Formal Reduction Potentials and the Entropy Effects for 1:1 Protein Complex. The formal reduction potentials of cytochrome *c* in different 1:1 protein complexes at 25 °C have similar values (Table 5). However, variations of the formal reduction potential with the temperature change for cytochrome *c* in different protein systems are different in magnitude (Table 6). The variation for individual cytochrome *c* alone from 10.8 to 41.8 °C is −36 mV, while the values for cytochrome *c* in different complex systems are −17, −26, −19, and −35 mV (i.e., Cyt *c*/Cyt *b*₅, Cyt *c*/Cyt *b*₅ E44A, Cyt *c*/Cyt *b*₅ E56A, and Cyt *c*/Cyt *b*₅ E44/56A, respectively). These results demonstrate that the different cytochrome *b*₅ species exert different effects on the mutual interaction with cytochrome *c* in the 1:1 protein complexes, consequently influencing the redox

behavior of cytochrome *c*. The wild-type Cyt *b*₅ has the strongest effect, and the Cyt *b*₅ E44/56A has the weakest effect. It does suggest that both Glu44 and Glu56 of cytochrome *b*₅ participate in the formation of 1:1 protein/protein complexes. As a result, the electrostatic interaction between cytochrome *c* and the wild type and E44A, E56A, and E44/56A of cytochrome *b*₅ should have an order as follows: Cyt *c*/Cyt *b*₅ > Cyt *c*/Cyt *b*₅ E56A > Cyt *c*/Cyt *b*₅ E44A > Cyt *c*/Cyt *b*₅ E44/56A. This result also indicates that the Glu44 has stronger electrostatic interaction with cytochrome *c* than the Glu56 does. On the other hand, looking at the wild type and E44A, E56A, and E44/56A of cytochrome *b*₅, their variations in the formal reduction potential from 10.8 to 41.8 °C are 23.5, 18.2, 19.3, and 17.5 mV, respectively. It implies that these different cytochrome *b*₅ species received similar effects from the mutual interaction with cytochrome *c*. The formal reduction potentials of cytochrome *b*₅ and its mutants at 25 °C in 1:1 protein complexes are compared with those measured in the single-protein systems (see Table 5); the differences are +8, −1, +3, and +1 mV for the wild type and E44A, E56A, and E44/56A proteins, respectively. The smaller changes in redox potential might imply that the mutual interaction of cytochrome *c* with the cytochrome *b*₅ species has little perturbation effect on the heme environment of cytochrome *b*₅, consequently leading to a limited effect on the reduction potentials of cytochrome *b*₅ variants. Comparatively, we concluded before that the Mg²⁺ ion plays a more important role in disturbing the heme environment of cytochrome *b*₅ than of the cytochrome *c* (23, 25).

The variations in entropy change of cytochrome *c* in the different protein systems are in the following order: Cyt *c*/Cyt *b*₅ > Cyt *c*/Cyt *b*₅ E56A > Cyt *c*/Cyt *b*₅ E44A > Cyt *c*/Cyt *b*₅ E44/56A (Table 5). Considering cytochrome *c* first, the strong interaction and the formation of a cytochrome *b*₅/cytochrome *c* protein complex results in a decrease in the net protein charges. The number of ordered water molecules surrounding cytochrome *c* also decreases with substitution by cytochrome *b*₅. These substituted water molecules are converted into the disordered state, and it should give rise to a positive entropy change. The same behaviors should be observed when Cyt *b*₅ E44A, Cyt *b*₅ E56A, and Cyt *b*₅ E44/56A are present instead of the wild-type cytochrome *b*₅, respectively. However, we observed the negative entropy changes in the above systems. This means that, as we suggested previously, the main contribution to the entropy changes upon reduction comes from the conformational change. The variations in magnitude should reflect the

Hydrogen bond network around Glu44 in cytochrome b_5 .

Glu44(A-O)	Arg47(A-H)	Arg47(A-O)	Ala50(A-H)
Glu43(A-O)	Leu46(A-H)	Gly42(A-O)	Val45(A-O)
His39(A-O)	Gly42(A-H)		

Hydrogen bond network around Glu56 in cytochrome b_5 .

Glu56(A-O)	Asp60(A-H)	Glu56(A-O)	Glu59(A-H)
Thr55(A-O)	Glu59(A-H)	Thr55(A-O)	Phe58(A-H)
Ala54(A-O)	Phe58(A-H)	Glu59(A-H)	Gly62(A-O)
Phe58(A-O)	His63(A-H)	Ser64	heme-propionate7

FIGURE 9: Hydrogen bond network around Glu44 (A) and Glu56 (B) in cytochrome b_5 .

strength of the mutual interaction between the proteins. So, the smaller negative entropy change of cytochrome c in the 1:1 protein systems upon reduction can be explained by the stronger bindings of cytochrome b_5 species to cytochrome c , leading to more of the surrounding water molecules being driven away from the surface of cytochrome c and/or inhibiting the conformational change of cytochrome c . According to this criteria, in the wild-type cytochrome b_5 /cytochrome c system, cytochrome c has the smallest entropy change because of the strongest mutual interaction; the

entropy change of cytochrome c in the Cyt c /Cyt b_5 E44A system is bigger than in the Cyt c /Cyt E56A system, which implies that the mutual interaction is reduced by mutation more at E44 than at E56, indicating that the former residue is more strongly involved in the mutual interaction between cytochrome c and cytochrome b_5 .

Now let us turn to cytochrome b_5 and its three mutants. As listed in the Table 5, the entropy changes of the proteins in the 1:1 complexes are the following: -63.4 , -53.3 , -50.3 , and -54.4 J/mol \cdot K for the wild type and for E44A, E56A, and E44/56A of cytochrome b_5 , respectively. This implies that for the three mutants, because they are more stable than the wild-type protein, cytochrome c induced smaller effects on their conformational changes. The difference of entropy changes between these values in 1:1 protein complex systems and those values in individual cytochrome b_5 proteins alone (i.e., -95.3 , -37.2 , -67.7 , and -31.3 J/mol \cdot K for the wild type and for E44A, E56A, and E44/56A of cytochrome b_5 , respectively) are $+31.9$, -16.1 , $+17.4$, and -23.1 J/mol \cdot K, respectively. It is noteworthy that both the Cyt b_5 E44A and the Cyt b_5 E44/56A show negative variations in entropy changes. Since the solvation effects on the entropy do not exhibit big differences as indicated before, it means that the presence of the positively charged cytochrome c stimulates more conformational changes on these two species, giving rise to more negative entropy changes. On the other hand, the positive variations in entropy changes exhibited by both the wild-type cytochrome b_5 and the Cyt b_5 E56A could be attributed to the strong interaction between the carboxylate of E44 and the amine group of lysine residue of cytochrome c , stabilizing the protein structures and reducing the conformational changes of cytochrome b_5 upon reduction. It indicates once again that the Glu44 plays a more important role in the formation of 1:1 Cyt c /Cyt b_5 complexes. These results are consistent with the results obtained from the analysis on cytochrome c in 1:1 protein complexes.

The Standard Enthalpy Changes of the Protein/Protein Systems. In previous sections, we have focused our efforts on interpreting the mutual interactions by the formal reduction potentials and the reaction center entropy changes, ΔS°_{rc} . Our continued interest in understanding the electron-transfer mechanism and these mutual interactions has led us to investigate further the thermodynamics of cytochrome c , cytochrome b_5 , and its three mutants. The entropy changes for the complete cell reaction adjusted to the NHE scale, ΔS° , were calculated from the following equation (21, 45, 56):

$$\Delta S^\circ = \Delta S^\circ_{rc} - 65.21 \text{ J/mol}\cdot\text{K} \quad (9)$$

and the standard Gibbs free energy changes, ΔG° , were determined from the formal reduction potential, E° (vs NHE) at 25 $^\circ\text{C}$. Consequently, the standard enthalpy changes, ΔH° , were obtained from the corresponding ΔG° and ΔS° according to eq 10:

$$\Delta G^\circ = \Delta H^\circ - T\Delta S^\circ \quad (10)$$

From Table 5 it is interesting to note that the Gibbs free energy of cytochrome c shows a similar driving force upon reduction on the electrode (the cytochrome c alone only shows a slight bias over in the other protein/protein systems). This is the same situation with cytochrome b_5 . However, if

you compare the ΔH° and the ΔS° , it is evident that cytochrome *c* feels more effect from the mutual interaction of cytochrome *b₅*, especially the wild type and E56A of cytochrome *b₅* (almost 20 kJ/mol of ΔH° changes and 60 J/mol·K of ΔS° changes). On the contrary, cytochrome *b₅* proteins experience much less effect from the interaction with cytochrome *c*, especially those mutant proteins (the ΔH° changes are about 4–8 kJ/mol and the ΔS° changes are within 20 J/mol·K). Once again, this indicates that cytochrome *c* suffers more intensive conformational changes in the cytochrome *c*/cytochrome *b₅* interaction than its partner, cytochrome *b₅*. In addition, the cytochrome *b₅* mutants experience less conformational changes because the proteins have already been more compacted by mutation. The fact that the entropy change of cytochrome *c* in Cyt *c*/Cyt *b₅* E44/56A complex, -110.0 J/mol·K, is very close to that of cytochrome *c* alone, -118.7 J/mol·K, does not imply that there is no electrostatic interaction between cytochrome *c* and Cyt *b₅* E44/56A, because its counterpart, Cyt *b₅* E44/56A in 1:1 protein complex presents very different entropy change from that of individual Cyt *b₅* E44/56A alone. It is plausible that some combination of protein conformational change and solvation effect is responsible for the observed thermodynamic behaviors. However, this requires further investigation.

All proteins studied here exhibit the negative standard enthalpy changes upon reduction. Several authors (28, 43, 45) have suggested that in cytochrome *c* the negative enthalpy implies a stable protein structure in the reduced state. They suggested that the length of the Fe–S bond in its reduced state of cytochrome *c* is shorter and brought about a more rigid and stable structure. Although we have no direct evidence, at the moment, to confirm whether the Fe–N bond in ferricytochrome *b₅* is also strengthened, the higher denaturation temperature of its reduced state in urea (Table 3) and the negative enthalpy changes for cytochrome *b₅* and its three mutants provide strong support for the same assumption. Cowan et al. (61) further suggested that the mechanism of more negative ΔH° values resulted from favorable d– π overlap between ferrous ion and heme ligand. The experimental results obtained here propose that the ferrocycytochrome *b₅* and its three mutants are more favorable for metal/ligand electronic interaction, because the Fe–N π back-bonding makes it more possible to form a stabilized N–Fe–N system with a decrease in Fe(II)–N bond length (21, 56).

From the study on the thermodynamic parameters of protein/protein interaction, it has been shown that the technique of cyclic voltammetry is sensitive to the conformational behavior of proteins as a function of temperature in the bulk solution. The interesting results reported by Roscoe et al. (62–63) also suggested that at various temperatures the conformational change in protein can alter their electrochemical property. The results obtained in the present paper, as well as Roscoe's reports, provide important insights into understanding the mutual interaction between proteins.

CONCLUSIONS

A series of comparative studies have been completed on the stability of the wild type and its three mutants of

cytochrome *b₅*. When the Glu44 and Glu56 were mutated to alanine, the stability of the protein increased slightly. The experimental results obtained either from the denaturation by urea or the heme dissociation upon heating, indicate that for the wild-type cytochrome *b₅* and its mutants, the order of stability is the following: wild type \sim E44A $<$ E56A $<$ E44/56A. Because the Glu44 and Glu56 are situated in two different hydrogen bond networks of cytochrome *b₅*, when these hydrophilic residues are changed to hydrophobic residues, alanine, disappearance of some hydrogen bonds and alteration of the force balance in protein structure result in the heme being more tightly held by two pairs of helices. Meanwhile, because the part of the protein molecule where the Glu44 is located is more flexible than the part of the molecule where the Glu56 is located, it is understandable that the influence of mutation at Glu56 on the stability of cytochrome *b₅* is bigger than at Glu44.

To elucidate the role that Glu44 and Glu56 of cytochrome *b₅* played in the electrostatic interaction between cytochrome *c* and cytochrome *b₅*, electrochemical studies by cyclic voltammetry were performed. From the temperature dependence of the formal reduction potential, a series of thermodynamic parameters of cytochrome *c*, cytochrome *b₅*, and its three mutants were determined. For each individual protein system studied here, we propose that the negative entropy changes mainly reflect the conformational changes upon reduction. As expected, for the 1:1 protein complex systems, because of the mutual interaction between cytochrome *c* and cytochrome *b₅* or its mutants, each protein in the protein complexes exhibits different entropy behavior with respect to that of the individual proteins alone. The difference in magnitude should reflect the strength of the mutual interaction between the two proteins in 1:1 protein complexes. In summary, the experimental results demonstrate that both the Glu44 and the Glu56 of cytochrome *b₅* are involved in the mutual interactions with cytochrome *c*; the Glu44 seems to play a more important role than Glu56 for the structure and function of cytochrome *b₅*.

The important effect of the mutual interaction on heterogeneous electron transfer, between cytochrome *c* and cytochrome *b₅* or its mutants, would greatly enhance the knowledge of the important biological redox components and its partners. It is hoped that this study will lead to a better understanding of the properties of the protein/electrode interface, as well as the effects of the protein mutual interaction on their electron-transfer reaction. It is also conceivable that such information would promote the prospects of developing a biosensor for observation of the nature of the cytochrome *c*, the cytochrome *b₅*, and its partners.

ACKNOWLEDGMENT

We gratefully acknowledge Professor A. G. Mauk of the University of British Columbia, Canada, for his kind gifts of the cytochrome *b₅* gene.

REFERENCES

1. Strittmatter, P., Spatz, L., Corcoran, D., Rogers, M. J., Setlow, B., and Redline, R. (1974) *Proc. Natl. Acad. Sci. U.S.A.* 71, 4565–4569.
2. Bonfils, C., Balny, C., and Maurel, P. (1981) *J. Biol. Chem.* 256, 9457–9465.

3. Hultquist, D. E., Sannes, L. G., and Juckett, D. A. (1984) *Curr. Top. Cell. Regul.* 24, 278–300.
4. Spatz, L., and Strittmatter, P. (1971) *Proc. Natl. Acad. Sci. U.S.A.* 68, 1042–1046.
5. Strittmatter, P., and Ozols, J. (1966) *J. Biol. Chem.* 241, 4787–4792.
6. Hultquist, D. E., Dean, R. T., and Douglas, R. H. (1974) *Biochem. Biophys. Res. Commun.* 60, 28–34.
7. Lloyd, E., Ferrer, J. C., Funk, W. D., Mauk, M. R., and Mauk, A. G. (1994) *Biochemistry* 33, 11432–11437.
8. Mathews, F. S., Argos, P., and Levine, M. (1971) *Cold Spring Harbor Symp. Quant. Biol.* 36, 387–395.
9. Durlay, R. C. E., and Mathews, F. S. (1996) *Acta Crystallogr., Sect. D* 52, 65–76.
10. Salemme, F. R. (1976) *J. Mol. Biol.* 102, 563–568.
11. Stayton, P. S., Poulos, T. L., and Sligar, S. G. (1989) *Biochemistry* 28, 8201–8205.
12. Poulos, T. L., and Mauk, A. G. (1983) *J. Biol. Chem.* 258, 7369–7373.
13. Pearce, L. L., Utecht, R. E., and Kurtz, D. M., Jr. (1987) *Biochemistry* 26, 8709–8717.
14. Livingston, D. J., McLachlan, S. J., La Mar, G. N., and Brown, W. D. (1985) *J. Biol. Chem.* 260, 15699–15707.
15. Mauk, M. R., Mauk, A. G., Weber, P. C., and Matthew, J. B. (1986) *Biochemistry* 25, 7085–7091.
16. Northrup, S. H., Thomasson, K. A., Miller, C. M., Barker, P. D., Eltis, L. D., Guillemette, J. G., Inglis, S. C., and Mauk, A. G. (1993) *Biochemistry* 32, 6613–6623.
17. Rodgers, K. K., and Sligar, S. G. (1991) *J. Mol. Biol.* 221, 1453–1460.
18. Sun, Y.-L., Xie, Y., Wang, Y.-H., Xiao, G.-T., and Huang, Z.-X. (1996) *Protein Eng.* 9(7), 555–558.
19. Hill, H. A. O. (1993) *Molecular Electrochemistry of Inorganic, Bioinorganic and Organometallic Compounds*, NATO ASL Series C, Vol. 385, pp 133–149.
20. Armstrong, F. A. (1990) *Structure and Binding*, Vol. 72, pp 139–221. Springer-Verlag, Berlin, Germany.
21. Taniguchi, V. T., Ellis, W. R., Jr., Cammarata, V., Webb, J., Anson, F. C., and Gray, H. B. (1982) *Electrochemical and Spectrochemical Studies of Biological Redox Components* (Kadish, K. M., Ed.) pp 51–58, American Chemical Society, Washington, D.C.
22. Huang, Z.-X., Feng, M., Wang, Y.-H., Cui, J., and Zou, D.-S. (1996) *J. Electroanal. Chem.* 416, 31–40.
23. Wang, Y.-H., Cui, J., Sun, Y.-L., Yao, P., Zhuang, J.-H., Xie, Y., and Huang, Z.-X. (1997) *J. Electroanal. Chem.* 428, 39–45.
24. Yao, P., Wang, Y.-H., Xie, Y., and Huang, Z.-X. (1998) *J. Electroanal. Chem.* 445, 197–201.
25. Qian, W., Zhuang, J.-H., Wang, Y.-H., and Huang, Z.-X. (1998) *J. Electroanal. Chem.* 447, 187–199.
26. Powell, R. E., and Latimer, W. M. (1951) *J. Chem. Phys.* 19, 1139–1141.
27. George, P., Hanania, G. I. H., and Irvine, D. H. (1954) *J. Chem. Phys.* 22, 1616.
28. Taniguchi, V. T., Sailasuta-Scott, N., Anson, F. C., and Gray, H. B. (1980) *Pure Appl. Chem.* 52, 2275–2281.
29. Sailasuta, N., Anson, F. C., and Gray, H. B. (1979) *J. Am. Chem. Soc.* 101, 455–458.
30. Hill, H. A. O. (1987) *Pure Appl. Chem.* 59(6), 743–748.
31. Bowden, E. F., Hawkrige, F. M., Chlebowski, T. F., Bancroft, E. E., Thorpe, C., and Blount, H. N. (1982) *J. Am. Chem. Soc.* 104, 7641–7644.
32. Brautigan, D. L., Ferguson-Miller, S., and Mergoliash, E. (1978) *Methods Enzymol.* 53D, 128.
33. Sun, Y.-L., Wang, Y.-H., Zhou, G., Huang, Z.-X., Xie, Y., and Wu, X.-Z. (1996) *Chem. J. Chin. Univ.* 17, 1673–1677.
34. Sanger, F., Nicklen, S., and Coulson, A. R. (1977) *Proc. Natl. Acad. Sci. U.S.A.* 74, 5463–5467.
35. La Mar, G. N., Toi, H., and Krishnamoorthi, R. (1984) *J. Am. Chem. Soc.* 106, 6395–6401.
36. Pace, C. N. (1986) *Methods Enzymol.* 131, 266–280.
37. Matthew, J. B., and Gurd, F. R. N. (1986) *Methods Enzymol.* 130, 437–453.
38. Matthews, C. R. (1987) *Methods Enzymol.* 154, 498–511.
39. Yee, E. L., Cave, R. J., Guyer, K. L., Tyma, P. D., and Weaver, M. J. (1979) *J. Am. Chem. Soc.* 101, 1131–1137.
40. Adams, P. L. (1977) *Biochem. J.* 163, 153–158.
41. Armstrong, F. A., Bond, A. M., Hill, H. A. O., Psalti, I. S. M., and Zoski, C. G. (1989) *J. Phys. Chem.* 93, 6485–6493.
42. Niles Mcleod, D. D., Freeman, H. C., Harvey, I., Lay, P. A., and Bond, A. M. (1996) *Inorg. Chem.* 35, 7156–7165.
43. Moore, G. R., and Williams, R. J. P. (1980) *Eur. J. Biochem.* 103, 523–532.
44. Taniguchi, I., Iseki, M., Eto, T., Toyasawa, K., Yamaguchi, H., and Yasukouchi, K., (1984) *Bioelectrochem. Bioenerg.* 13, 373–383.
45. Taniguchi, I., Funatsu, T., Iseki, M., Yamaguchi, H., and Yasukouchi, K. (1985) *J. Electroanal. Chem.* 193, 295–302.
46. Willit, J. L., and Bowden, E. F. (1990) *J. Phys. Chem.* 94, 8241–8246.
47. Lin, T., and Breck, W. G. (1965) *Can. J. Chem.* 43, 766–771.
48. Matthew, J. B. (1993) *Annu. Rev. Biochem.* 62, 139–160.
49. Caffrey, M. S., and Cusanovich, M. A. (1991) *Biochemistry* 30, 9238–9241.
50. Durlay, R. C. E., and Mathews, F. S. (1991) Brookhaven Protein Data Bank, entry 3b5c.
51. Hunter, C. L., Lloyds, E., Eltis, L. D., Rafferty, S. P., Lee, H., Smith, M., and Mauk, A. G. (1997) *Biochemistry* 36, 1010–1017.
52. Jiang, S.-K., Wu, H.-M., Yao, P., Wang, Y.-H., Xie, Y., and Huang, Z.-X. (1998) Comparative Study on the Structures of the Trypsin-solubilized Recombinant Cytochrome *b₅* and F35Y Mutant in Solution by 2D NMR. (submitted to *Biochem. J.* for publication).
53. Sun, Y.-L., Jiang, S.-K., Wu, H.-M., and Huang, Z.-X. (1998) Comparative study of 2D NMR and electron-transfer reaction on the recombination cytochrome *b₅* and its E44/56A variant. (submitted to *J. Mol. Biol.* for publication).
54. Newbold, R. J., Hewson, R., and Whitford, D. (1992) *FEBS Lett.* 314, 419–422.
55. Yao, P., Wang, Y.-H., Sun, Y.-L., Xie, Y., and Huang, Z.-X. (1997) *Protein Eng.* 10(5), 575–581.
56. Taniguchi, V. T., Malmstrom, B. G., Anson, F. C., and Gray, H. B. (1982) *Proc. Natl. Acad. Sci. U.S.A.* 79, 3387–3389.
57. Caffrey, M. S., and Cusanovich, M. A. (1994) *Biophys. Acta* 1187, 277–288.
58. Koller, K. B., and Hawkrige, F. M. (1985) *J. Am. Chem. Soc.* 107, 7412–7417.
59. Koller, K. B., and Hawkrige, F. M. (1988) *J. Electroanal. Chem.* 239, 291–306.
60. Reid, L. S., Taniguchi, V. T., Gray, H. B., and Mauk, A. G. (1982) *J. Am. Chem. Soc.* 104, 7516–7519.
61. Lui, S. M., and Cowan, J. A. (1994) *J. Am. Chem. Soc.* 116, 11538–11549.
62. Roscoe, S. G., Fuller, K. L., and Robitaille. (1993) *J. Colloid. Interface Sci.* 160, 243–251.
63. Hanrahan, K. L., MacDonald, S. M., and Roscoe, S. G. (1996) *Electrochim. Acta* 41(15), 2469–2479.

BI9805036